

SPLIT-CHANNEL RECTANGULAR AIRLIFT REACTORS: ENHANCEMENT OF PERFORMANCE BY GEOMETRIC MODIFICATIONS

K. H. CHOI, Y. CHISTI* and M. MOO-YOUNG

*Department of Chemical Engineering, University of Waterloo,
Waterloo, Ontario, Canada N2L 3G1*

(Received September 22, 1994; in final form April 26, 1995)

Two geometric configurations of gas–liquid separators were used in split-channel airlift reactors (0.1 m³ liquid volume; riser-to-downcomer cross-sectional area = 1.45; aspect ratio = 3.6) to test the effect of geometry on hydrodynamic performance and oxygen transfer behaviour. One of the configurations consisted of the basic internal-loop airlift head region without added features; the other had a 45°-inclined prism attached to the upper edge of the splitting baffle. For otherwise fixed conditions, the design of gas–liquid separators affected the induced liquid circulation velocity, the depth of penetration of the bubbles in the downcomer, the gas holdup in the downcomer and the mixing time. The overall volumetric gas–liquid oxygen transfer coefficient was not affected. The gas holdup in the riser was only marginally affected by the design of the separator; however, the relationship between the riser and the downcomer holdups was sensitive to separator configuration. Incorporation of the prism in the basic airlift configuration enhanced gas–liquid separation so much so that up to 30% reduction in the downcomer gas holdup could be obtained relative to the unmodified geometry. The impact of the separator designs on hydrodynamic behaviour could be explained as emanating from a combination of the gas–liquid separating ability of the design and its hydraulic resistance.

KEYWORDS Airlift reactor Gas–liquid separator Hydrodynamics Oxygen transfer

INTRODUCTION

The many attractive features of airlift reactors have led to increasing usage of these devices in environmental remediation technology, the chemical process industry and the biotechnology-based manufacture (Chisti, 1989; Chisti and Moo-Young, 1987; Onken and Weiland, 1983). Airlift reactors have an established niche in high-strength activated sludge type treatment of wastewater where the high oxygen transfer capability, low power requirements and nonmechanical agitation are particular advantages of these systems (Chisti, 1989; Redman, 1987; Varey, 1992). Bioremediation of soil fines in airlift devices is being investigated as a promising new pollution abatement application of this technology (Chisti and Moo-Young, 1994). Similarly, applications in treatment of gaseous effluents are expected (Moo-Young and Chisti, 1994).

An airlift reactor consists of a riser and a downcomer that are interconnected near the top and the bottom of the reactor as shown in Figure 1. The riser is usually sparged with a gas, commonly air. The downcomer is usually not aerated. Differential aeration

* Author to whom all correspondence should be addressed.

bubbles in the downcomer, the relationship between the riser and the downcomer gas-holdups, mixing characteristics, the induced liquid circulation velocity and the overall volumetric oxygen transfer coefficient are investigated.

EXPERIMENTAL

The reactors used consisted of a Plexiglas vessel with a rectangular cross-section divided into a riser and downcomer by a vertical baffle as shown in Figure 1. The reactors differed only in the configuration of the head region. Two configurations were investigated: a basic internal-loop head region without special features for gas-liquid separation as in Figure 2a and a configuration with a 45° -inclined prism attached to the upper edge of the vertical baffle (Figs. 1 and 2b). In both cases, the cross-sectional area ratio of downcomer-to-riser was 0.689. The unaerated liquid heights were equal at 1.64 m. Because the prism occupied some volume and the aspect ratios were identical for the two cases, liquid volume in the reactors differed slightly. The volumes were 0.106 and 0.108 m^3 , respectively, for the configuration with and without the prism. The riser was sparged with air through a perforated plate sparger located at its base. The sparger had 30 holes, 0.002 m in diameter, drilled on $0.0445 \times 0.0255 \text{ m}$ rectangular pitch. The reactors were designed to prevent accumulation of solids at the base of the downcomer in possible future applications. Thus, the base was inclined at an angle of 60° to the horizontal to ensure that the flow would sweep any sedimented particles into the riser where they could be resuspended by the upward flow of the slurry (Figure 1).

Tap water and air were the liquid and the gas phase, respectively. The air flow rates were measured by a calibrated rotameter and the superficial gas velocity, based on the cross-sectional area of the riser, varied over $0.017\text{--}0.135 \text{ m s}^{-1}$. Batch operation was employed with respect to the liquid phase. All experiments were carried out at room temperature and atmospheric pressure.

The gas holdups in the riser and the downcomer were determined manometrically (Chisti, 1989). The riser and the downcomer each had manometric taps located at 0.45 and 1.35 m above the base plate. Inverted water manometers were used.

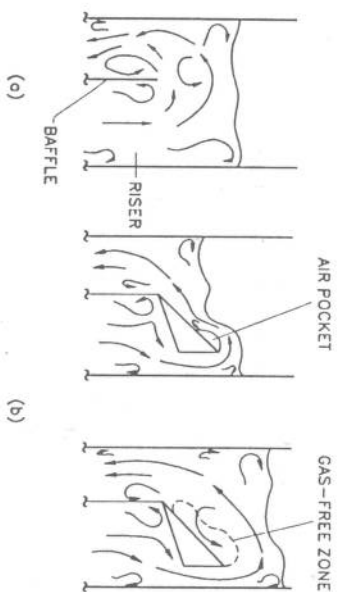


FIGURE 2 Configurations of the head region: (a) without prism; (b) with a 45° -inclined prism at low (left) and high gas flow rates.

The velocity of liquid circulation was determined with the neutral buoyancy flow follower technique. A small piece of plastic tube (0.0095 m in outer diameter, 0.02 m long and 1.022 in specific gravity) was used as a flow follower. The time taken by the follower to traverse a known vertical distance in the downcomer was noted and the flow velocity was calculated from an average of 10–20 measurements.

The mixing time was measured by the tracer impulse method (Chisti, 1989). Sodium hydroxide (2 M) and sulfuric acid (1 M) solutions (2 ml each) were alternately injected into the top of the downcomer as tracers. The variations in pH were monitored with a pH probe, pH meter and chart recorder arrangement. The pH probe was installed 0.40 m above the gas sparger in the downcomer. The mixing time was calculated from the response curves as the time required to achieve 90% of the final tracer concentration.

The overall volumetric oxygen transfer coefficient, $k_L a_L$, was determined by the dynamic gassing-in method as used previously by Chisti and Moo-Young (1988). A polarographic dissolved oxygen electrode (Yellow Springs, YSI 5739) and a dissolved oxygen meter (YSI model 57) were used to follow the change in concentration of oxygen in a batch of liquid that had previously been freed of oxygen by bubbling through with nitrogen. The mass transfer coefficient data here have been corrected to a common temperature of 20°C using equation (Rand *et al.*, 1975).

$$(k_L a_L)_{20} = \frac{(k_L a_L)_T}{(1.024)^{T-20}}, \quad (1)$$

where the subscripts T and 20 denote values at any measurement temperature T and at 20°C, respectively.

RESULTS AND DISCUSSION

For otherwise identical conditions, the rate of circulation of liquid in airlift reactors can be enhanced by reducing the gas holdup in the downcomer; hence, increasing the driving force for liquid circulation. Two main methods of reducing the downcomer holdup have been described (Chisti and Moo-Young, 1993): Either the cross-sectional area of the entrance to the downcomer in the head zone of the reactor may be enlarged so that the downward superficial velocity of the liquid in this zone is reduced sufficiently that entrainment of gas bubbles is eliminated; or, the distance between the entrance of the downcomer and the exit of the riser may be lengthened so that the bubbles have sufficient time to rise out of the liquid before it recirculates. While both these methods can be used with either the external- or the internal-loop airlift configurations, the latter technique is the more common for the external-loop devices (Bello, 1981; Chisti, 1989; Mao *et al.*, 1992). When gas-liquid separation is desired in internal-loop reactors, expanded downcomer entrances are the usual method of attaining it. However, expanded downcomers lead to cumbersome head regions as described elsewhere (Chisti and Moo-Young, 1993). To avoid this, an usual reactor configuration incorporating a 45°-inclined prism was used in this work to enlarge the cross-sectional area of the entrance of the downcomer.

The visually observed flow patterns in the two configurations of the head region are depicted in Figure 2. In configuration a (Fig. 2), a local liquid circulation zone occurred just inside the downcomer, close to the upper edge of the baffle. As the liquid flow velocity increased, the flow separated from the edge of the baffle and a pocket of air, attached to the upper edge, formed inside the downcomer. Similar observations were previously reported (Choi *et al.*, 1995) in a split-channel rectangular airlift device, which, unlike the present configuration, had a downcomer that was larger than the riser ($A_d/A_r = 1.45$). In contrast to the previous report, the size of the circulation zone and the air pocket in the present configuration a were smaller. In configuration b, at low values of the riser superficial gas velocities ($U_{gr} \leq 0.034 \text{ m s}^{-1}$), an air pocket attached to the upper surface of the prism formed in the downcomer entrance (Fig. 2). A small liquid circulation zone existed in the riser where the prism was attached to the vertical baffle. As the gas flow rate increased, the air pocket disappeared and was replaced by a zone of circulating liquid (dashed lines in Fig. 2b) that was not penetrated by the gas bubbles. Disappearance of the pocket was caused by the increasing hydrostatic pressure above the prism as more liquid moved into the head zone with increasing aeration rate and the level of the dispersion rose. Size of the liquid circulation zone near the edge of the vertical baffle was small in comparison with configuration a. Even at larger gas flow rates ($U_{gr} > 0.035 \text{ m s}^{-1}$) a distinct step change was noticeable in the levels of gas-liquid dispersion above the riser and the downcomer (Fig. 2b). The upward directed high velocity stream of liquid issuing from the narrow exit of the riser caused this effect. Visual observations confirmed configuration b to be an effective gas-liquid separator.

As illustrated in Figure 3, the gas holdup in the riser was little affected by the configuration of the head region; however, the holdup in the downcomer was strongly affected. As expected, configuration a (Fig. 2) was the less effective gas-liquid separator and allowed a greater carry-over of the gas bubbles into the downcomer, thus producing a higher downcomer gas holdup for any given conditions (Fig. 3). In comparison with previously published data for a configuration having a larger

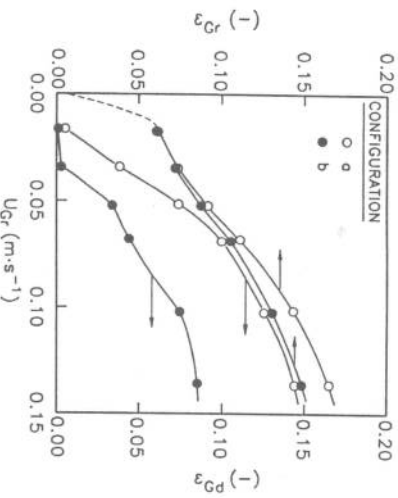


FIGURE 3 Effects of the geometry of the head region on fractional gas holdups in the riser (ϵ_g) and the downcomer (ϵ_{gd}).

downcomer than the riser (Choi *et al.*, 1995), the present configuration a allowed greater recirculation of the gas into the downcomer. This was because, with the downcomer cross-sectional area smaller than that of the riser, the downward superficial liquid velocity in the entrance of the downcomer was relatively high and able to drag a correspondingly larger number of bubbles into the downcomer. Configuration b was a better gas-liquid separator; hence, the downcomer gas holdup was lower with this design (Fig. 3). As is clear in Figure 3, over most of the range of operating gas velocity, the difference between the riser and downcomer gas holdups was larger for configuration b. Thus, the driving force for liquid circulation was proportionately larger. Yet, in Figure 4, the superficial liquid velocity in the downcomer of configuration b exceeded that in the riser only when the superficial gas velocity was about 0.04 m s^{-1} or greater. Note in Figure 3 that, while the driving force for liquid circulation was initially large for configuration a, it declined with increasing gas velocity as more bubbles went into the downcomer. Correspondingly, in Figure 4, the rate of induced liquid circulation obtained with configuration a showed a rapid initial rise, but soon plateaued. In configuration b, although the driving force for circulation was large throughout (Fig. 3), the liquid flow rate was initially lower than in design a because of the higher pressure drop characteristics of configuration b. Eventually, the better gas-liquid separating ability of configuration b did lead to higher induced liquid circulation rate.

Working with draft-tube internal-loop airlift reactors, Bello (1981) empirically obtained the following linear relationship between the riser and the downcomer gas holdups:

$$\varepsilon_{Gd} = 0.89 \varepsilon_{Gr} \quad (2)$$

A comparison of Eq. (2) with the data for configuration a is shown in Figure 5. Equation (2) is seen to breakdown for low values of riser gas holdup as has also been pointed out

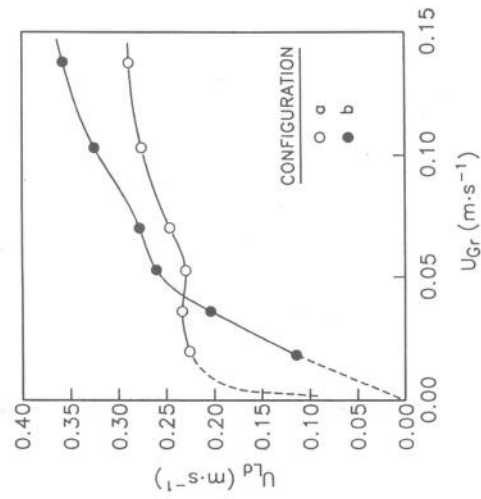


FIGURE 4 Effects of the geometry of the head region on the induced superficial liquid velocity (U_{Ld}) in downcomer.

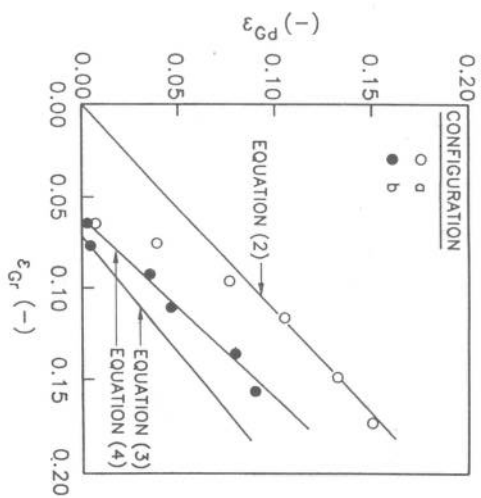


FIGURE 5 Relationship between the gas holdup in the riser and the downcomer.

elsewhere (Chisti *et al.*, 1995). The data for configuration b are located well below the prediction of Eq. (2) which was developed for reactors without gas-liquid separators (Fig. 5). As seen in Figure 5, configuration b is an effective gas-liquid separator compared to configuration a. However, compared to external-loop airlift reactors in which the relationship between the riser and the downcomer gas holdups has been determined (Bello, 1981) to be

$$\epsilon_{Gd} = 0.79 \epsilon_{Gr} - 0.057, \quad (3)$$

the configuration b is less effective (Fig. 5). Data for configuration b followed the equation

$$\epsilon_{Gd} = 1.029 \epsilon_{Gr} - 0.066. \quad (4)$$

The effects of the geometry of the head region on bubble penetration depth in the downcomer are shown in Figure 6 as a function of the superficial gas velocity in the riser. For the purpose of this work, the bubble penetration depth (H_p) is defined as the distance from the top of the vertical baffle to the bubble layer front in the downcomer. Although, for both configurations, very small bubbles (approximately < 2 mm diameter) did recirculate through the downcomer, such recirculation was disregarded in measurements of the bubble penetration depth. The latter referred to penetration of bubbles larger than about 3 mm. As shown in Figure 6, the bubble penetration depth increased as the gas velocity increased. Similar results were reported by Choi *et al.* (1995) for other configurations of split-channel airlift reactors. For configurations a and b, at sufficiently large values of the gas velocity, the bubble front could reach the bottom of the vertical baffle. Recirculation of gas was achieved beyond this critical gas velocity as observed also by Choi *et al.* (1995).

The rapid rise in bubble penetration depth that accompanied the initiation of gas flow in configuration a (dashed line in Figure 6) attested to the relatively low pressure

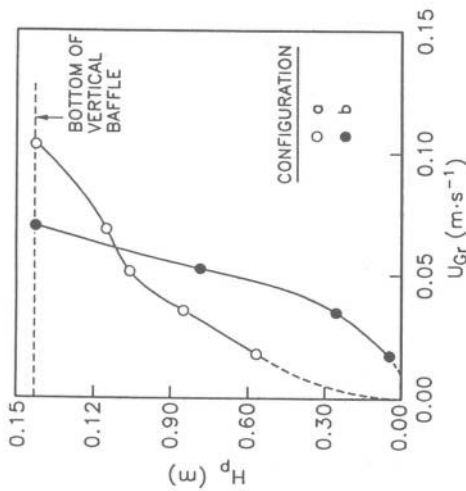


FIGURE 6 Effects of the geometry of the head region on the depth of penetration (H_p) of the bubble front in the downcomer.

drop offered by this configuration. Thus, slight increase in gas flow rate caused a large increase in liquid circulation rate (see also Figure 4); an earlier onset of bubble flow into downcomer occurred and the bubbles penetrated deeper into the downcomer. Although, because of high initial liquid velocity and poor gas-liquid separation, deeper penetration of gas bubbles initially occurred in configuration a, the faster rise in penetration depth with increasing gas flow rate in configuration b ensured that complete penetration of the downcomer occurred earlier in configuration b. The higher downward liquid flow, because of better gas-liquid separation in design b, was responsible for this effect.

The effect of the geometry of the head zone on mixing time are shown in Figure 7. In keeping with the expected general trend (Choi *et al.*, 1995), the mixing time decreased with increasing superficial gas velocity in configuration b. Results in configuration a were unusual, but reproducible. Increasing gas flow rate up to about 0.05 m s^{-1} increased mixing time (Fig. 7) while the liquid circulation rate remained constant (Fig. 4). Further increase in gas velocity caused small increase in liquid circulation rate and a corresponding improvement in mixing. Visual observations showed that the liquid circulation zones in the riser and the entrance of the downcomer (Fig. 2a) grew in size as the gas flow rate increased to about 0.05 m s^{-1} . These zones became unstable and growth ceased with further increase in gas velocity. For $U_{Gr} > 0.05 \text{ m s}^{-1}$, interchange of fluid between the bulk circulating stream and the circulating 'dead-zones' improved. These visual observations were consistent with the behaviour of the mixing time curve.

The data on the overall volumetric oxygen transfer coefficient for the two configurations are presented in Figure 8. In contrast to previously published data in reactors with downcomer cross-sectional areas that were larger than the riser (Choi *et al.*, 1995), no significant difference between the performance of the two configurations was noticed. In both cases, as the superficial gas velocity increased, the overall volumetric

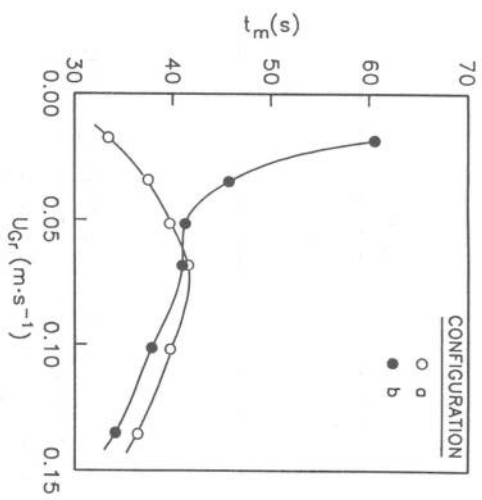


FIGURE 7 Effects of the configuration of the head region on mixing time (t_m).

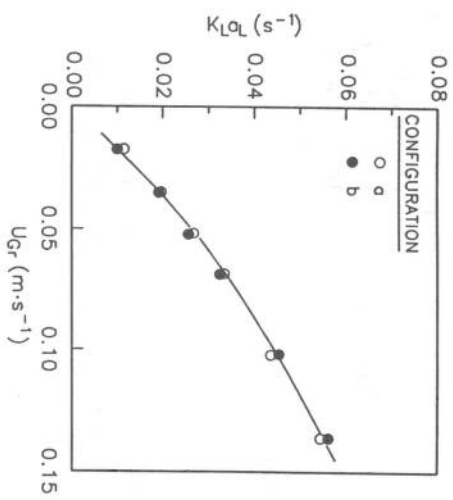


FIGURE 8 Effects of the configuration of the head region on the overall volumetric oxygen transfer coefficient ($k_L a_L$).

oxygen transfer coefficient, $k_L a_L$, increased because of an increase in the overall gas holdup and, hence, an increase in the gas-liquid interfacial area for oxygen transfer. The oxygen transfer coefficient data could be correlated with the superficial gas velocity using the equation:

$$k_L a_L = \alpha U_{Gr}^\beta \quad (5)$$

The values of α and β for the two configurations are summarized in Table 1.

TABLE I

Constants in Eq. (5) for the Two Configurations of the Head Region

Configuration	α	β
a	0.2405	0.7357
b	0.2772	0.7918

CONCLUSION

The hydrodynamic and aeration performance of split-channel internal-loop airlift reactors was shown to depend on the geometric configuration of the gas-liquid separator zone. For otherwise fixed conditions—aspect ratio of reactor, riser-to-downcomer cross-sectional area ratio and operational gas velocity—the performance characteristics, including the velocity of the induced liquid circulation, gas holdup in the downcomer, depth of penetration of the bubble front in downcomer and mixing time could be manipulated through design of the head zone. The gas holdup in the riser and the overall volumetric gas-liquid oxygen transfer coefficient were not sensitive to the geometry of the head region. The effects of any geometric configuration on performance characteristics could be explained as originating from a combination of the gas-liquid separating ability of the configuration and its resistance to liquid flow. Empirical correlations were proposed for estimation of the overall volumetric oxygen transfer coefficient in air-water system. The relationship between the riser and the downcomer gas holdups was established.

ACKNOWLEDGEMENTS

This work was funded by the Natural Sciences and Engineering Research Council of Canada. One of the authors (KHC) was supported by the Korea Science and Engineering Foundation.

NOMENCLATURE

H_p	Bubble penetration depth, m
$k_L a_L$	Overall volumetric oxygen transfer coefficient, s^{-1}
T	Temperature, $^{\circ}C$
t_m	Mixing time, s
U_{Gr}	Superficial gas velocity based on riser cross-sectional area, ms^{-1}
U_{Ld}	Superficial liquid velocity in downcomer, ms^{-1}
α	Coefficient in equation (5), $m^{-\beta} s^{\beta-1}$
β	Exponent in Eq. (5)
ϵ_{Gd}	Gas holdup in downcomer
ϵ_{Gr}	Gas holdup in riser

REFERENCES

- Bello, R. A., A Characterization Study of Airlift Contactors for Application to Fermentations, Ph.D. Thesis, University of Waterloo, Ontario, Canada (1981).
- Chisti, Y., *Airlift Bioreactors*, Elsevier Applied Science, London (1989).
- Chisti, Y., and Moo-Young, M., Airlift Reactors: Characteristics, Applications and Design Considerations, *Chem. Eng. Commun.*, **60**, 195-242 (1987).
- Chisti, Y., and Moo-Young, M., Hydrodynamics and Oxygen Transfer in Pneumatic Bioreactor Devices, *Biotechnol. Bioeng.*, **31**, 487-494 (1988).
- Chisti, Y., and Moo-Young, M., Improve the Performance of Airlift Reactors, *Chem. Eng. Progress*, **89**(6), 38-45 (1993).
- Chisti, Y., and Moo-Young, M., Airlift Bioreactors for Treatment of Hydrocarbon Contaminated Wastes, in: *Better Living Through Biochemical Engineering*, W. K. Teo, M. G. S. Yap and S. K. W. Oh, (eds.), University of Singapore, Singapore, pp. 771-776 (1994).
- Chisti, Y., Wenge, F., and Moo-Young, M., Relationship Between Riser and Downcomer Gas Holdup in Internal-Loop Airlift Reactors without Gas-Liquid Separators, *Chem. Eng. J.*, **57**, B7-B13 (1995).
- Choi, K. H., Chisti, Y., and Moo-Young, M., Influence of the Gas-Liquid Separator Design on Hydrodynamic and Mass Transfer Performance of Split-Channel Airlift Reactors, *J. Chem. Technol. Biotechnol.*, **62**, 327-332 (1995).
- Mao, H. H., Chisti, Y., and Moo-Young, M., Multiphase Hydrodynamics and Solid-Liquid Mass Transport in an External-Loop Airlift Reactor—a Comparative Study, *Chem. Eng. Commun.*, **113**, 1-13 (1992).
- Moo-Young, M., and Chisti, Y., Bioreactor Applications in Waste Treatment, *Res. Cons. Recycl.*, **11**, 13-24 (1994).
- Onken, U., and Weiland, P., Airlift Fermenters: Construction Behaviour and Uses, *Adv. Biotechnol. Proc.*, **1**, 67-95 (1983) Alan R. Liss, New York.
- Rand, M. C., Greenberg, A. E., and Taras, M. J., (eds.), *Standard Methods for the Examination of Water and Wastewater*, 14th Ed., American Public Health Association, Washington, p. 87, 1975.
- Redman, J., Deep Shaft Treatment for Sewage, *Chemical Engineer (Lond.)*, **441**, 12-13 (1987).
- Varey, P., Airlift for Purity, *Chemical Engineer (Lond.)*, **529**, s37 (1992).

